



# Effect of Diwali Firecrackers on Air Quality and Aerosol Optical Properties over Mega City (Delhi) in India

M. Sateesh<sup>1</sup> · V. K. Soni<sup>2</sup> · P. V. S. Raju<sup>1</sup>

Received: 11 February 2018 / Accepted: 29 May 2018 / Published online: 6 June 2018  
© Springer International Publishing AG, part of Springer Nature 2018

## Abstract

In this paper, the variations of aerosol properties due to crackers burning during Diwali event (11th–18th 2012) over mega city Delhi were investigated. The sky radiometer POM-2 aerosol optical property data from Skynet-India along with ambient air pollution data were critically analyzed. The aerosol optical depth (AOD) at 500 nm was 1.60 on 13th November, the Diwali day, and its value a maximum of 1.84 on 16th November. Due to stable atmosphere over Delhi during post Diwali, aerosols accumulate and remain in the atmosphere for longer time, which leads to higher AOD on 16th November. A lower value of single-scattering albedo (SSA) was observed at a longer wavelength (1020 nm) during the entire period that clearly indicates the dominance of absorbing-type black carbon aerosol. SSA showed a steep decrease after 16th November. Asymmetry parameter decreased to a maximum of 0.79 for the shorter wavelength at 340 nm and 0.632 is reported at the higher wavelength 1020 nm. Asymmetry parameter showed a decrease in value just after Diwali on 14th November, this suggesting the dominance of fine-mode aerosol from anthropogenic activities. The lowest value of the refractive index (1.4527) on 14th and 15th November indicates the higher loading of absorbing-type aerosol which may be associated with firecracker burning of Diwali festival. The significant correlation with the value of  $r=0.9$  was observed between sky radiometer and MODIS AOD with a standard deviation of 0.31 and an RMSE of 0.17 during the event. Radiative forcing and heating rate were estimated using SBDART. The maximum average concentrations 2641 and 1876  $\mu\text{g}/\text{m}^3$  of PM<sub>10</sub> and PM<sub>2.5</sub>, respectively, were observed on the Diwali night. A highest of 109 ppb surface ozone was reported in the night at 23:00 IST, which can be attributed to burning of the firecrackers.

**Keywords** AOD · Air pollution · PM<sub>2.5</sub> · MODIS and HYSPLIT back trajectory

## 1 Introduction

In recent years, concerns for atmospheric aerosols have been increased due to their adverse effects on regional air quality, human health, weather, and climate. Numerous studies have been carried out to assess the anthropogenic aerosols especially in densely populated mega cities. During the recent time, firing cracker is getting popularity especially in urban regions which leads to substantial air pollution and degradation of visibility (Singh et al. 2015). The burning of crackers is a major source of pollution in India during Diwali

festival (Pervez et al. 2016; Pongpiachan et al. 2017). Firecrackers emit a huge amount of gaseous pollutants such as carbon monoxide, ozone, sulfur dioxide, and nitrogen oxides (Attri et al. 2001). Burning of firecrackers also release a large quantity of particulate matter along with several metal salts (such as Pb, Cd, V, Ni, Cu, Zn, Mn, and Fe) into the atmosphere, which forms dense clouds of smoke containing various toxic compounds (Kulshrestha et al. 2004; Pöschl 2005; Aksu 2015). The studies on elevated concentrations of pollutants during celebrations with firecrackers are very few in Indian context (Barman et al. 2008; Chatterjee et al. 2013; Darga et al. 2006; Devara et al. 2015; Simha et al. 2013). Firecrackers cause acute short-term air quality degradation (Barman et al. 2008), but long-term effects on regional climate (Ramanathan and Feng 2009), long- and short-term effects on human health (Godri et al. 2010), and also visibility reduction (Clark 1997). A recent study on UK Guy Fawkes Nights affected the visibility during the

✉ P. V. S. Raju  
pemmani@gmail.com; pvsraju@jpr.amity.edu

<sup>1</sup> Centre for Ocean-Atmospheric Science and Technology,  
Amity University Rajasthan, Jaipur, India

<sup>2</sup> India Meteorological Department, Lodi Road, New Delhi,  
India

festival period (Singh et al. 2015). The higher wind speeds will washout/drifted the aerosol concentrations, clear sky conditions increases the planetary boundary layer in the noon time, and the higher relative humidity conditions will produce hazy conditions in the early morning hours. The inverse relation between RH and visibility will affect the optical properties of aerosol (Singh et al. 2017). The surface ozone concentrations are proportional to temperatures where as these ozone concentrations are high in the night time also in the presence of NO<sub>2</sub>, NO, and fluorescence emitting firecrackers.

The urban air database released by the World Health Organization in September 2011 reported that Delhi has already exceeded the maximum PM<sub>10</sub> limits. The increase of PM<sub>10</sub> and PM<sub>2.5</sub> is affecting the human health in terms of respiratory problem which leads to chronic diseases (Nidhi and Jayaraman 2007) over high dense metropolitan cities such as National Capital Regions (NCR), India. This becomes a serious issue in the point of public health; the government of India has taken an initiative to ban firecrackers in and around the NCR to prevent the usual spike in toxic air pollution levels. Aerosols are tiny particles suspended in the atmosphere and exhibit a range of sizes depending on the source of production (smoke particles, dust, fog, etc.). These particles are responsible for scattering or absorption of solar radiation within the atmosphere. The characterization of the spectral dependence of AOD in the atmosphere is imperative for modeling of the radiative effects of aerosols (Ali et al. 2017; Eck et al. 1999).

Diwali is one of the historical festivals celebrated in India during the post monsoon season of October/November every year. During the Diwali festival, millions of people light traditional lamps and burn firecrackers especially in north India. The firecrackers are low intensity explosive pyrotechnic devices which can be classified as handheld, ground based, and aerial firecrackers. It is normally celebrated for three consecutive days. The preparations for festival celebrations start by burning firecrackers a few days before the Diwali and reach an upsurge on the Diwali day. The firecrackers continue after Diwali for few more days. During the year 2012, the main day of Diwali was on 13th November.

In this paper, we have presented variations in aerosol characteristics from satellite remote sensing measurements and ground-based observation during the Diwali festival period 11th–18th November 2012. The temporal variations of gaseous pollutants, solar-radiation flux, and meteorological parameters were also studied. Correlation of these elevated perturbations in aerosol parameters with other plausible meteorological parameters and effects on radiative forcing were discussed. The main reason for selecting 2012 Diwali is prevailing cloud-free sky that during the period is ideal case to investigate the aerosol optical properties in detail. However, the aerosol concentrations are high in the

cloudy conditions as compared to the cloud-free conditions due to the lowering of PBL which can be examined by the active sensors such as Lidar, CALIPSO observations (Deng et al. 2016). The CALIPSO observations on these Diwali days over Pune region also show an increase of back scatter coefficient at 5 km (Devara et al. 2015).

The present study will help understand the effect of acute transient air pollution episode and further improves air quality predictions, as currently available models do not incorporate the air pollution data arises from the firecrackers under cloud-free condition.

## 2 Data and Methodology

Delhi is the national capital territory of India, located between the latitudes of 28° 24'–28° 53' N and longitudes of 76° 50'–77° 20' E, (218 m, AMSL), having an area of 1483 km<sup>2</sup>. Delhi is considered as one of the most polluted urban regions, lies in the Indo-Gangetic plain where anthropogenic activities are more. The air quality in November month is poor over northern parts of India due to the extreme crop residue burning episodes along with vehicular and industrial pollution. The winds from the north-west direction will bring the smoke to the Indo-Gangetic plain; furthermore, it affects the air quality and visibility (Dumka et al. 2016; Kharol et al. 2012; Mor et al. 2017).

Sky radiometer (POM-02), an automatic sun-tracking equipment capable of measuring direct solar and diffuse sky irradiance at different spectrums ranging from ultra violet region to near Infrared region, is used for the measurement of aerosol optical properties in Delhi. The columnar aerosol optical parameters such as aerosol optical depth (AOD), single-scattering albedo (SSA), and asymmetry parameter (ASY) are derived from the sun/sky irradiance measurements at seven wavelengths, i.e., 315, 400, 500, 675, 870, 940, and 1020 nm using Beer–Lambert law. More details of instrument configuration, data collection, calibration, and inversion algorithms of sky radiometer are provided in (Nakajima et al. 1996). The time series of optical and physical properties of columnar aerosol is discussed during the Diwali event. The Aqua satellite-based MODIS 3 km aerosol product (MYD04\_3K) at 550 nm (Nichol and Bilal 2016) has also been used for comparison studies over Delhi. The daytime averaged aerosol optical depth (AOD) measured by the sky radiometer (POM-II) is compared with the MODIS-3 km (MYD04\_3K) satellite data over Delhi region to find the temporal correlation during the period.

In general, the aerosol particle distribution categorized into three types based on their size are nucleation (Aitken) mode (particle diameter < 0.1 µm), a fine/accumulation mode (particle diameter: 0.1 µm < *d* < 1 µm), and a coarse mode (particle diameter *d* > 1 µm) (Bisht et al. 2015). The

spectral dependence of AOD has been used to derive aerosol volume size distribution in the vertical column of the atmosphere using inversion algorithm (Nakajima et al. 1996). The observed aerosol columnar volume size distribution is found to be a bimodal lognormal function represented by

$$\frac{dV}{d \ln r} = \frac{V_0}{\sigma 2\pi} \exp \left\{ -\frac{\ln \left( \frac{r}{r_m} \right)^2}{2\sigma^2} \right\}, \quad (1)$$

where  $V_0$  denotes the particle volume concentration,  $r_m$  is the median radius, and  $\sigma$  is the standard deviation.

PM10 and PM2.5 concentrations were monitored using Beta Attenuation Monitor (BAM-1020), which employs the principle of beta-ray attenuation. Surface ozone concentration was measured with a UV ozone photometer model Thermo-49i. Concentration of NO and NO<sub>x</sub> was measured with chemiluminescence NO<sub>x</sub> analyzers model Thermo-42i. Carbon monoxide (CO) in ambient air was measured using the gas filter correlation method by CO Analyzer Model Thermo-48i. A detailed description of monitoring methods and site locations is also available in Parkhi et al. (2016), and these instruments are well calibrated on real time to give public awareness (<http://safar.tropmet.res.in>). The meteorological data presented in this study were obtained from India Meteorological Department.

### 3 Results and Discussion

The aerosol loading in the atmosphere is significantly influenced by the meteorological conditions (Shaw 1988). Figure 1a represents the average daily variations of meteorological parameters such as air temperature (°C), relative humidity (%), pressure (hPa), and wind speed (kmph) during Diwali festive period. The daily average temperature, relative humidity, and pressure varied from 16–20 °C, 55–78%, and pressure range (1014–1017) hPa, respectively, over Delhi during Diwali period (Fig. 1a). The daily average temperature reported lowest on Diwali day (13th November) with minimum value of 16.3 °C. It is further increased to 17.3 °C on 14th November. The daily average relative humidity started increasing from 11th November and reached a maximum of 78% on 12th November, after that RH showed decreases till 15th November. The high RH during these high pollution episodes leads to the reduction of visibility by changing its optical properties (Singh et al. 2015, 2017). Prior to Diwali, slightly lower wind speed is observed, whereas the higher wind speed was observed during Diwali and post Diwali period. But there is an abrupt decrease in wind speed on 16th November, which leads to calm condition and stable atmosphere. The diurnal

variations of outgoing terrestrial radiation from 11th to 18th November over Delhi are depicted in Fig. 1b. The diurnal variation of solar radiative flux measured at every 10 min interval using pyranometer was higher (366 W m<sup>-2</sup> day<sup>-1</sup>) compared to other days (260–290 W m<sup>-2</sup> day<sup>-1</sup>).

#### 3.1 Spectral Variations of AOD

Figure 2a depicts the daily spectral variations of mean AOD during the Diwali festival period over Delhi. The vertical bar signifies the standard deviation of the daily mean AOD at each wavelength. The mean AOD at 500 nm measured from sky radiometer depicts lesser value 0.75 on 18th November 2012, demonstrating that the atmosphere was relatively less on that day compared to other days of festive period. AOD increases from the prior to the Diwali. Since people start burning firecrackers about 2 days prior to the Diwali day and after 2 days especially in urban cities (Singh et al. 2004). On 13th November, the Diwali day AOD at 500 nm was 1.60 and it reached to a maximum value of 1.84 on 16th November (Fig. 2a). Spectral variability in AOD showed decreases with increasing wavelength during the whole study period. Highest values of AOD at all wavelengths were observed on 16th November which clearly indicates the higher aerosol loading after the festival. The loading of airborne trace metals is the main reason to increase AOD in the festival periods. A study carried by Kulshrestha et al. (2004) reported that Ba, K, Al, and Sr increase to 1090, 25, 18, and 15 times, respectively, to the previous Diwali day over a coastal site Chennai.

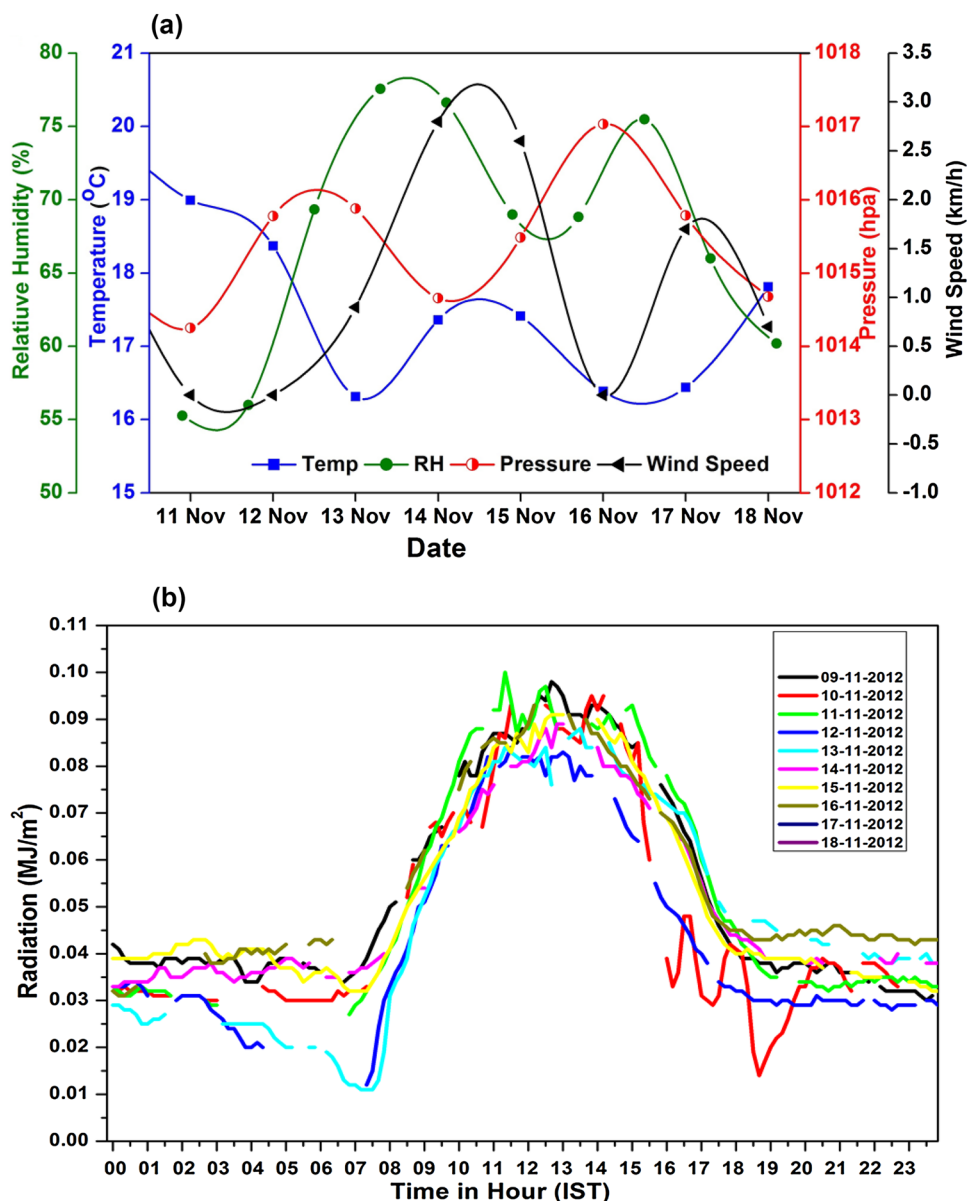
Ground-based measurements of AOD at 500 nm is extrapolated to obtain AOD at 550 nm (Ali et al. 2017; More et al. 2013) as per the mentioned formula (1) and compared with MODIS-derived values

$$\tau_{550} = \tau_{500} \left[ \frac{550 \text{ nm}}{500 \text{ nm}} \right]^\alpha. \quad (2)$$

From Fig. 2b, nearly similar tendency was observed in the MODIS/AQUA AOD at 550 nm. The difference in the observations is because MODIS data are at a specific time and spatially averaged, while sky radiometer data are point measurements. MODIS daily AODs at 550 nm were noticed in the range 0.43–1.44 during Diwali. The AOD at 550 nm was ~1.35 on the main Diwali day. MODIS AOD showed good agreement with sky radiometer-derived AOD. Figure 2c is the Taylor diagram showing correlation coefficient of 0.9 and centered root-mean-square error of 0.17 between MODIS AOD and sky radiometer measured AOD. The standard deviation of sky radiometer observed AOD is 0.37.

Figure 3a exhibits a distinct bimodal distribution similar to lognormal curves during Diwali period. The bimodal nature of the aerosol volume size distribution can be attributed to aerosols from a combination of different

**Fig. 1** **a** The daily averaged meteorological parameters and **b** diurnal variation of the outgoing terrestrial radiation



sources in the atmosphere (Hoppel et al. 1985). In general, the primary peak represented by the concentration of fine- and accumulation-mode particulates is due to the anthropogenic activities (Devara et al. 2015) and gas phase to particle reaction products (Singh et al. 2004). The secondary peak represents coarse-mode particles from natural sources such as wind blown dust (More et al. 2013). Figure 3a reveals that the fine-mode concentration was more after the Diwali period from 14th to 16th November 2012. This indicates the influence of smaller particles emitted from the Diwali firecrackers. After Diwali on 14th November 2012, there is high volume of fine-mode aerosol while a very low volume of coarse-mode aerosol clearly indicates the dominance of firecrackers burning fine-mode aerosols. The higher fine-mode concentration was observed

on 16th November 2012, whereas the lowest concentration of fine particles was reported on 18th November 2012. Table 1 shows the parameters of the accumulation- and coarse-mode radii of the aerosol columnar volume size distribution and corresponding values of the Angstrom exponent and turbidity coefficient. From Fig. 3a, we perceive that the fine-mode peak concentrations of aerosol particles range from 0.01 to 0.14  $\mu\text{m}$  with corresponding mean radius around  $\sim 0.5 \mu\text{m}$ , while coarse-mode aerosol particles are 1.1–10  $\mu\text{m}$  with corresponding mean effective radius as  $\sim 5 \mu\text{m}$  (Table 1). Nevertheless, in comparable studies, the magnitudes of coarse-mode peak volume concentration are slightly greater than fine-mode peak volume concentration during Diwali period.

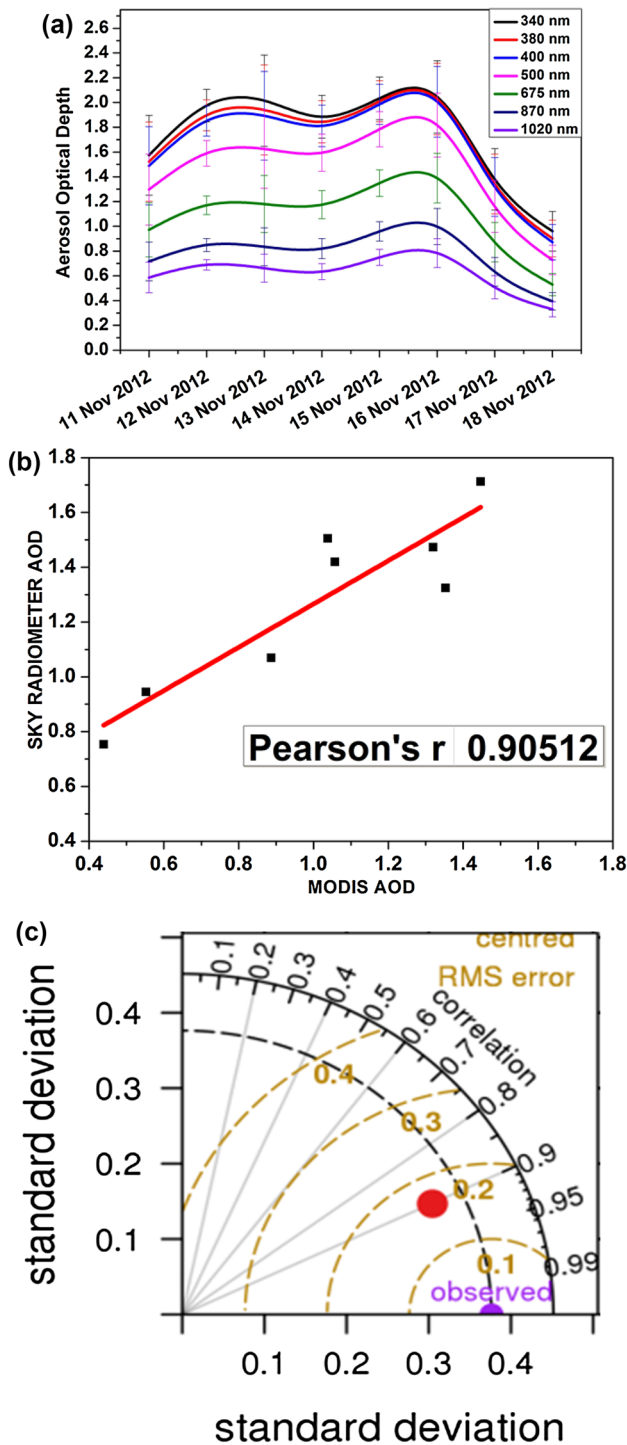


**Fig. 2** **a** Spectral AOD observed from sky radiometer. **b** Scattered plot between observed AOD and the MODIS-derived AOD at 550 nm. **c** Taylor diagram for the MODIS and sky radiometer observed AOD at 550 nm during Diwali period

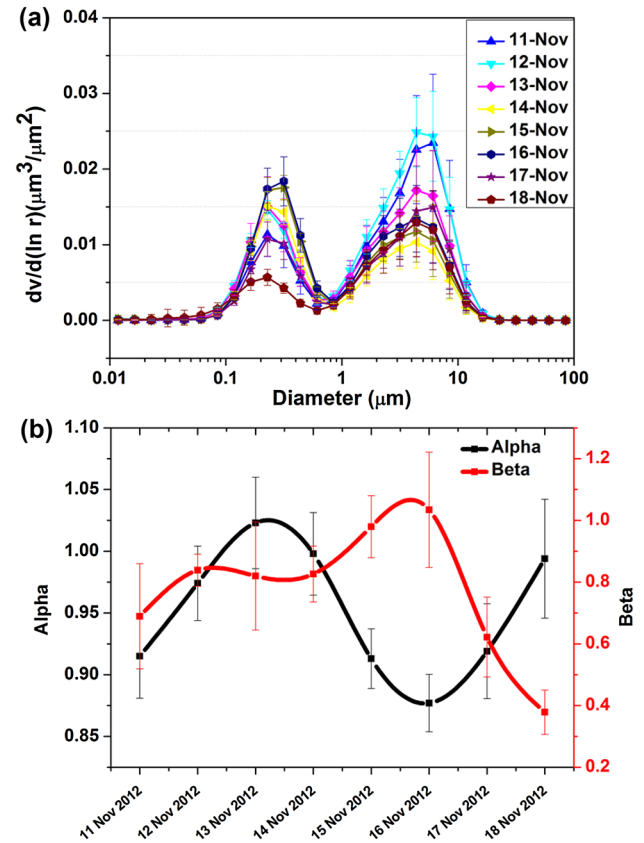


**Fig. 3** **a** Volume size distribution and **b** time series of alpha and beta

### 3.2 Aerosol Size Distribution

Angstrom exponent provides useful information on columnar aerosol size distribution and can be derived from spectral dependence of AOD at different wavelengths by fitting an Angstrom's power law (Angstrom 1964)

$$\tau_a = \beta \lambda^{-\alpha}, \quad (3)$$

where  $\tau_a$  is AOD,  $\beta$  is turbidity coefficient which is equivalent to the AOD measured at 1  $\mu\text{m}$ , and it vary 0–0.5; higher value of turbidity coefficient indicates higher aerosols loading (McCartney and Hall 1977).  $\alpha$  is the Angstrom exponent and its value varies from greater than 2.0 for accumulation-mode fresh smoke particles to nearly zero for high AOD desert dust events dominated by coarse-mode particles (Kaufman et al. 1992). The variations of  $\alpha$  and  $\beta$  are shown in Fig. 3b. Higher  $\alpha$  values indicates abundance of smaller particles, and relatively higher  $\beta$  implying more extinction is observed during 12th–14th November, when firecracker activities are at maximum. The observed magnitude of Angstrom exponent and turbidity coefficient was in the ranges 0.97–1.02 and 0.82–0.83, respectively, during 12th–14th November.



**Table 1** Volume concentration and effective radius of fine- and coarse-mode particles during Diwali event

	Fine mode			Coarse mode			Alpha	Alpha (SD)	Beta	Beta (SD)
	Volume concentration	$R$ ( $\mu\text{m}$ )	SD	Volume concentration	$R$ ( $\mu\text{m}$ )	SD				
11th November	0.036	0.611	0.005	0.080	5.448	0.027	0.915	0.0341	0.6893	0.1705
12th November	0.045	0.581	0.005	0.087	5.301	0.027	0.974	0.0301	0.8388	0.0519
13th November	0.044	0.544	0.005	0.061	5.194	0.027	1.023	0.037	0.8199	0.1751
14th November	0.040	0.467	0.004	0.037	4.965	0.026	0.998	0.0334	0.8261	0.0906
15th November	0.048	0.486	0.005	0.043	4.956	0.026	0.913	0.0242	0.9799	0.1004
16th November	0.050	0.506	0.005	0.050	5.010	0.026	0.877	0.0232	1.0345	0.1866
17th November	0.032	0.556	0.005	0.052	5.411	0.027	0.919	0.0384	0.6220	0.1297
18th November	0.023	0.637	0.006	0.046	5.087	0.026	0.994	0.0481	0.3786	0.0719

Angstrom exponents and turbidity coefficient are also presented

SSA is a fraction of the aerosol light scattering over the extinction, and it is a crucial variable in assessing the radiative effects of aerosols (Dubovik and King 2000; Jacobson 2000). For radiative forcing estimates, the top of the atmosphere (TOA) forcing strongly depends on SSA values (Takemura and Nakajima 2002). SSA characterizes the combined effect of scattering and absorption properties of aerosols. The spectral dependence of scattering coefficient is attributed to the size of particles and the absorption coefficient to chemical composition of the particles. Thus, SSA is mostly dependent on the size distribution and chemical composition of aerosols.

Figure 4a displays the variation of spectral SSA during the Diwali period. It is observed that SSA decreases with wavelength having a value of 0.95 at 380 nm and 0.93 at 1020 nm on 14th November 2012. Lower SSA at longer wavelength shows higher concentrations of absorbing-type black carbon aerosol, which is attributed to the presence of a mixture of aerosols from Diwali firecrackers. The higher change in SSA after the Diwali can be due to the prevailing meteorological conditions and the background urban aerosol concentrations.

The asymmetry parameter ( $g$ ) is a representation of cosine of the scattered angle for the scattered radiation and is a very sensitive optical property to controlling the aerosol radiative forcing. The variation of  $g$  with wavelengths is a representation of the angular scattering, and it depends on the size and composition of the particles. The value of  $g$  ranges between  $-1$  for entirely backward scattered radiation and  $+1$  for entirely forward scattered radiation. The scattering of the light by aerosols occurred when the size of the particle is higher than the wavelength of interacting radiation; most of the radiation will get scattered in the forward direction ( $0$  to  $+1$ ) and vice versa. The asymmetry factor varies with wavelengths due to that the sizes of aerosols are comparable with wavelengths of interacting radiation. Figure 4b shows temporal variations of daily asymmetry

parameter during Diwali festival 2012. The mean asymmetry factor during the period had a value varied from  $0.68 \pm 0.03$  to  $0.73 \pm 0.04$  at 500 nm. The 340, 870, and 1020 nm-based asymmetry parameters are showing minimum value on 14th November 2012, but the rest (i.e., 500, 675, and 400 nm) are showing on 13th November 2012. Lower value of  $g$  on 14th November is corresponding to dominance of fine-mode aerosol due to firecrackers burning during Diwali.

The size and chemical compositions of aerosols present in the atmosphere are important components for estimating the radiative effects of the aerosols. The refractive index (RI) is the best representation of the chemical composition of aerosols or absorbing type of aerosols (Torres et al. 1998) described by combining real  $n(\lambda)$  and imaginary  $k(\lambda)$  parts. The real part  $n(\lambda)$  denotes the scattering which leads to cooling while the imaginary part  $k(\lambda)$  enumerates the nature of the absorption which leads to warming of the atmosphere (Zarzana et al. 2012). In the present study, the refractive index of aerosols is derived using sky radiometer (Nakajima et al. 1996). The temporal variations of real and imaginary parts of the refractive index [ $n(\lambda)$  and  $k(\lambda)$ ] at 380 nm which has strong absorption of UV rays are shown in Fig. 4c. The  $n(\lambda)$  and  $k(\lambda)$  at 380 nm were 1.4527 and  $-0.0061$ , respectively, on 14th November 2012. The  $k(\lambda)$  decreased sharply from 13th to 14th November which implies that the absorption particles are dominant than the scattered particles. Thus, the aerosol particles emitted during the Diwali festival are more absorbing in nature, which was also confirmed from SSA values observed during festival period.

### 3.3 Long-Range Transport of Aerosols

Air mass back trajectories are often used to investigate the possible transport pathways of trace gases and atmospheric aerosols (White et al. 2006). These back trajectories are primarily intended from the observed meteorological fields. In this study, back trajectories are derived from

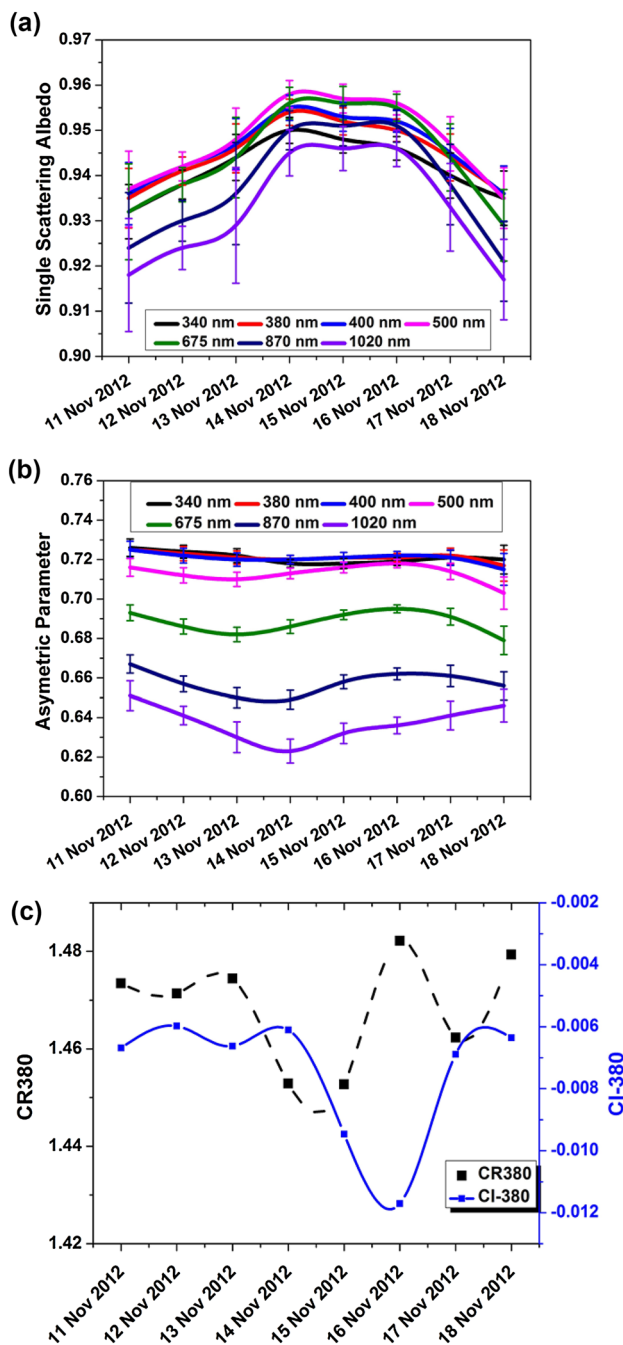


**Fig. 4** Variation of **a** single-scattering albedo, **b** asymmetry parameter, and **c** refractive index during the Diwali period. The vertical bars denote the  $1\sigma$  standard deviation from the mean values

National Oceanic and Atmospheric Administration Hybrid Single-Particle Lagrangian Integrated Trajectory (NOAA HYSPLIT) version 4 model (Draxler 1998). Figure 5 shows 5-day back trajectories over Delhi. A close examination of these trajectories demonstrated that all the air masses have their origin mostly over the northern states of Haryana, Punjab, Himachal Pradesh, and Pakistan, where the highest

biomass burning occurs during November. The biomass burning aerosols also significantly influenced the observed AOD during Diwali period. Images taken from MODIS Terra showed the hazy atmospheric conditions due to biomass burning and Diwali firecrackers over Delhi (Fig. 5d–f). High levels of pollution found over Delhi during Diwali were due to not only the local emissions from firecrackers, but also long-range transport of pollutants from Diwali firecrackers as well as biomass burning.

As the data sample size is small and the observations are limited to daytime only, segregation of increase in aerosol loading due to local meteorology, long-range transport, and Diwali festival activity is not possible in the present analysis. Figure 6 shows the MODIS (MYD04\_3k) Dark Target Deep Blue-derived AOD (Nichol and Bilal 2016) values over northern parts of India. The high AOD was observed over north-west part of India. The widespread increase in AOD values was observed on 12th and 13th November 2012. During the October and November months, biomass (mainly crop residue) burning is reported in northern parts of India. The increase in AOD and other pollutants has been reported by researchers due to the crop residue burning in the north-western parts of India (Badarinath et al. 2010; Bisht et al. 2015; Sharma et al. 2010). The widespread higher AOD values on 13th and 14th November over north-west part of India are due to firecrackers in addition to the effect of biomass burning.

The time series of PM concentration (PM<sub>2.5</sub> and PM<sub>10</sub>) at various locations in national capital city of Delhi is depicted in Fig. 7. The unprecedented rise in the PM<sub>2.5</sub> concentration values during the Diwali indicates the increase in the fine-mode particles in the atmosphere contributed by firecrackers. The concentration of PM<sub>10</sub> also showed significant rise at all the location during Diwali event. The increment in the particulate matter during Diwali contributes to rise in AOD, which lasts for several days after the festival till 16th November 2012 (Fig. 7a, b). Furthermore, the significant increase of NO<sub>x</sub>, NO<sub>2</sub>, CO, and O<sub>3</sub> at various locations over Delhi is also observed during Diwali period (Fig. 8).

The secondary pollutant, surface ozone, is produced in the presence of nitrogen oxides and sun light. Significant increase in surface ozone concentration was observed in the absence of sunlight (night time) during Diwali. The color emitting due to firecrackers burning will give light which can react with NO during the night time Diwali period to produce O<sub>3</sub>. A strong correlation of 0.993 is found during the Diwali nights with O<sub>3</sub> and NO in the presence of firecrackers (Attri et al. 2001). A highest concentration of 109 ppb was reported during night time at 23:00 IST, whereas the NO<sub>x</sub> and NO<sub>2</sub> were 63.7 and 23.2 ppb, respectively, on 14th November 2012 (Fig. 9). An average of 38 ppb is reported during the 18:00 IST

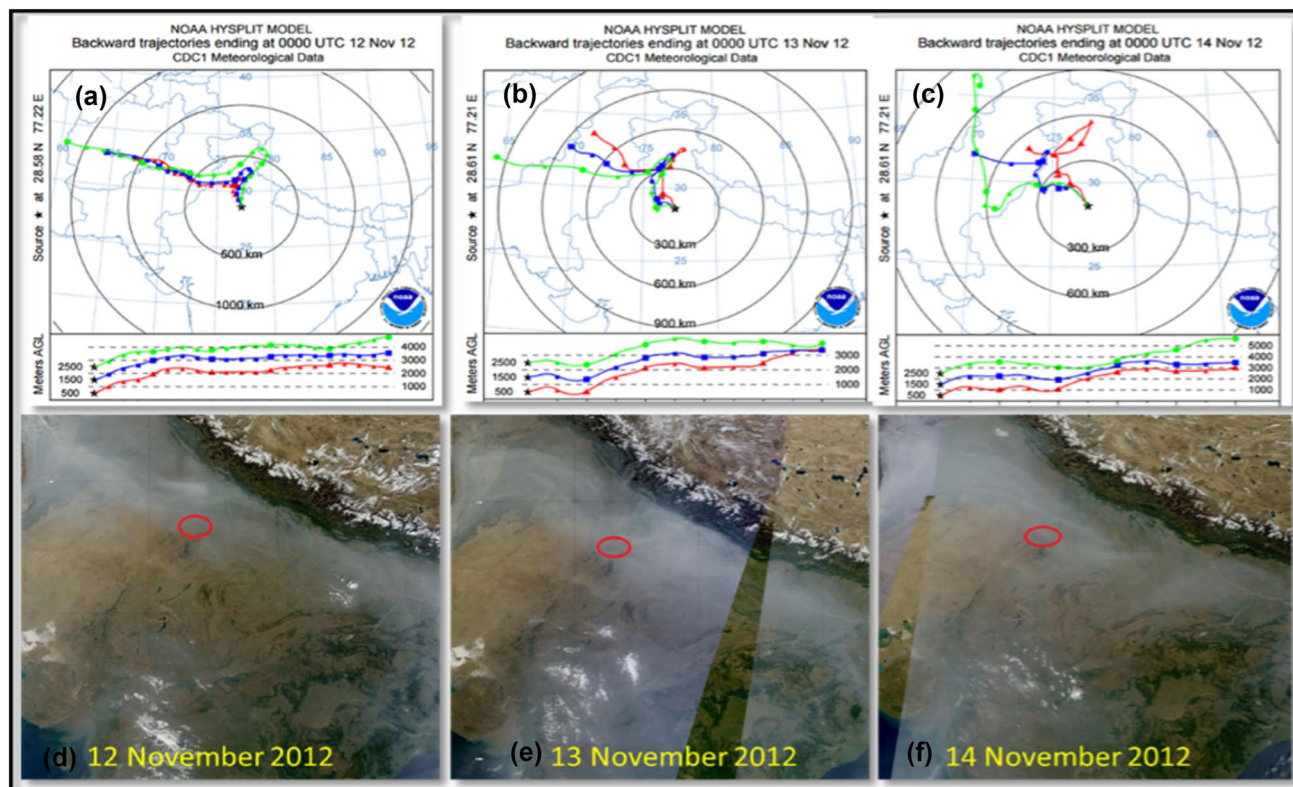


**Fig. 5** 5-day HYSPLIT back trajectory at three different altitudes 500 m (red color), 1500 m (blue color), and 2500 m (green color) during Diwali period **a** 12th November 2012, **b** 13th November 2012,

**c** 14th November 2012 over Delhi. Modis (Terra images), **d** 12th November 2012, **e** 13th November 2012, and **f** 14th November 2012

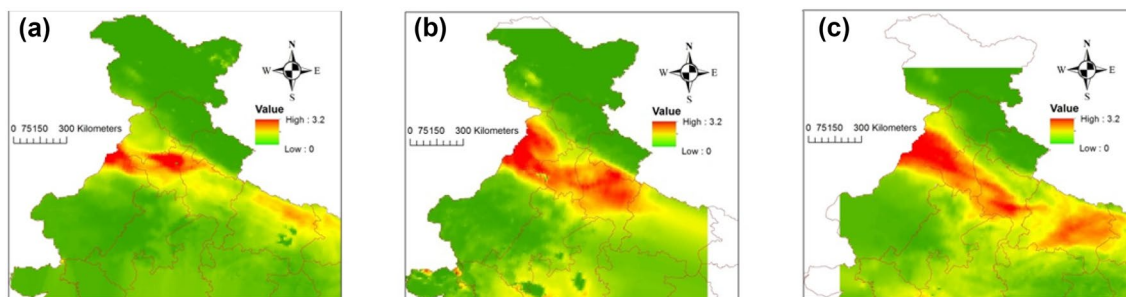


**Fig. 6** **a** MODIS-3 K AOD on 12th November 2012. **b** MODIS-3 K AOD on 13th November 2012. **c** MODIS-3 K AOD on 14th November 2012

(evening) to the next day morning 06:00 IST. When the firecrackers are burnt, a considerable proportion of light is radiated by its constituents in wavelength 240 nm which helps in producing surface ozone. Figure 9 shows two clusters, which may be due to the dependence of production of ozone with weather parameters or any other secondary gases. It can be resolved by considering a large number of observation points and detailed analysis in future studies.

### 3.4 Aerosol Radiative Forcing

SBDART is a plane-parallel radiative transfer model (Ricchiuzzi et al. 1988), used in various atmospheric studies by scientific communities for estimation of ARF. The parameters used as inputs in SBDART are AOD, SSA, Angstrom exponent, asymmetry parameter, and atmospheric profiles. In present, the daily mean values of AOD, SSA, and ASP at 500 nm wavelength from sky radiometer are used as inputs



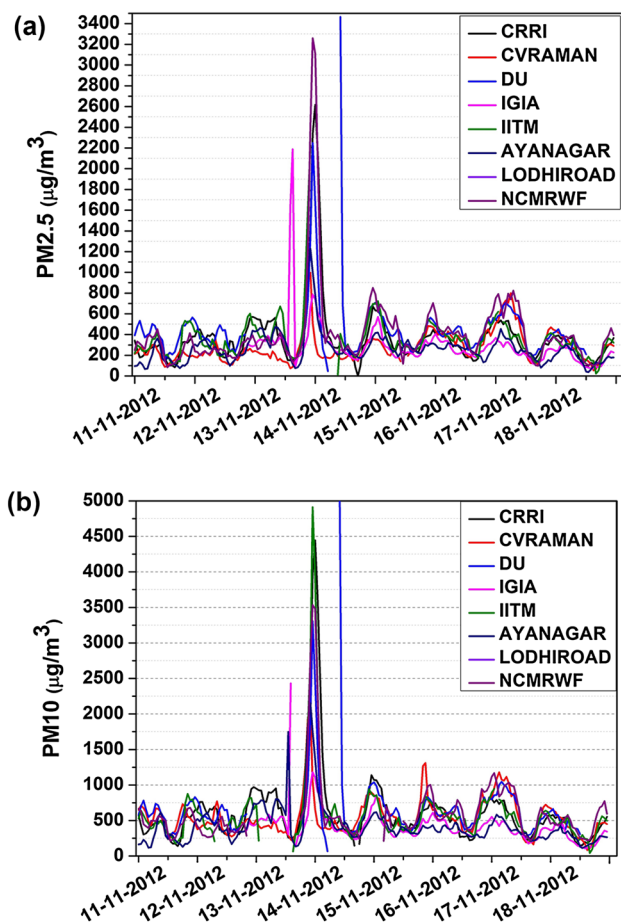


Fig. 7 Time series of **a** PM<sub>2.5</sub> and **b** PM<sub>10</sub>

to SBDART model. For accurate estimation of ARF, an input of surface albedo is an important parameter which was calculated using the MODIS satellite generated black-sky albedo (BSA) (direct reflectance) and white-sky albedo (WSA) (bi-hemispherical reflectance) at short wavelength spectral bands. Based on BSA and WSA at different solar zenith angles, the actual albedo was calculated as given below:

$$\text{Actual Albedo} = \text{WSA} * \text{DSF} + \text{BSA}(1 - \text{DSF}), \quad (4)$$

where DSF is diffuse sky fraction (DSF) which is a function of solar zenith angle and aerosol loading. The observed average AOD at its solar zenith angle has been used to derive DSF available from MODIS land team (Schaaf et al. 2002). MODIS-derived perceptible water content and OMI-derived total column ozone were also used as input parameters to SBDART.

In this study, ARF was calculated at the surface (SUR), top of the atmosphere (TOA), and within the atmosphere (ATM)

$$\text{ARF} = [F_{\text{down}} - F_{\text{up}}]_{\text{with aerosol}} - [F_{\text{down}} - F_{\text{up}}]_{\text{without aerosol}} \quad (5)$$

The net flux is difference of downward flux ( $F_{\text{down}}$ ) and upward flux ( $F_{\text{up}}$ ). The SBDART model computations are estimated at 30-min intervals on each day and daily average ARF values are estimated for TOA, SUR, and ATM.

Figure 10 shows the temporal variation in ARF along with the standard deviations obtained over Delhi during Diwali festive period. From Fig. 10, it is clear that during Diwali period, the SUR has negative forcing (cooling) while the ATM has positive forcing (warming). The average ARF for the entire period of observations at the surface was  $-53 \text{ Wm}^{-2}$  and at top of the atmosphere was  $-26 \text{ Wm}^{-2}$ , giving rise to an atmospheric forcing of about  $+27 \text{ Wm}^{-2}$ . ARF values observed over Kanpur (Kaskaoutis et al. 2013) at the SUR ( $-69$  to  $-97 \text{ Wm}^{-2}$ ), TOA ( $-20$  to  $30 \text{ Wm}^{-2}$ ), and ATM ( $+43$  to  $71 \text{ Wm}^{-2}$ ) were less than the value observed over in the present study. The ARF values on Diwali day, i.e., 13th November 2012 at SUR, TOA, and ATM were  $-61$ ,  $-30$ , and  $31 \text{ Wm}^{-2}$ , respectively. The average heating rate of  $1.8^\circ\text{C/day}$  was estimated for study period. The higher atmospheric heating in Diwali days is mainly due to lowered SSA associated with the Diwali firecrackers activities. The ARF values clearly indicate the substantial reduction in solar-radiation reaching Earth's surface and heating of the atmosphere during the period of the festival celebrations. Similar results of higher atmospheric heating with additional warming is observed as  $+12 \text{ Wm}^{-2}$  during fire crackers burning over Varanasi (Singh et al. 2014).

## 4 Conclusions

The aerosol properties and its distribution depend on the type of pollutant present in the atmosphere. The combination of biomass burning and the firecrackers impact fine-mode particles in the atmosphere on the Diwali day, and coarse-mode particles are more after the Diwali day. Higher aerosol loading was observed after Diwali with maximum value on AOD (1.84) on 16th November at 500 nm; this clearly indicates the effect of crackers burning. Asymmetry parameter showed decreasing pattern from shorter to longer wavelength during the entire study period with minimum value on 14th November. Volume size distribution showed a dominance of the fine-mode particles after the Diwali period from 14th to 16th November 2012, suggesting the more contribution of fine-mode particles emitted from the Diwali firecrackers. The air quality observations reveal the significant rise of ozone levels in the during night time which can be attributed to burning of firecrackers. The increment of PM<sub>2.5</sub> and PM<sub>10</sub> during the festival time contributes to the rise of optical parameters such as AOD and also warming in the atmosphere. The ARF values on Diwali day, i.e., 13th November 2012 at SUR, TOA, and ATM were  $-61$ ,  $-30$ , and  $31 \text{ Wm}^{-2}$ , respectively. The average heating

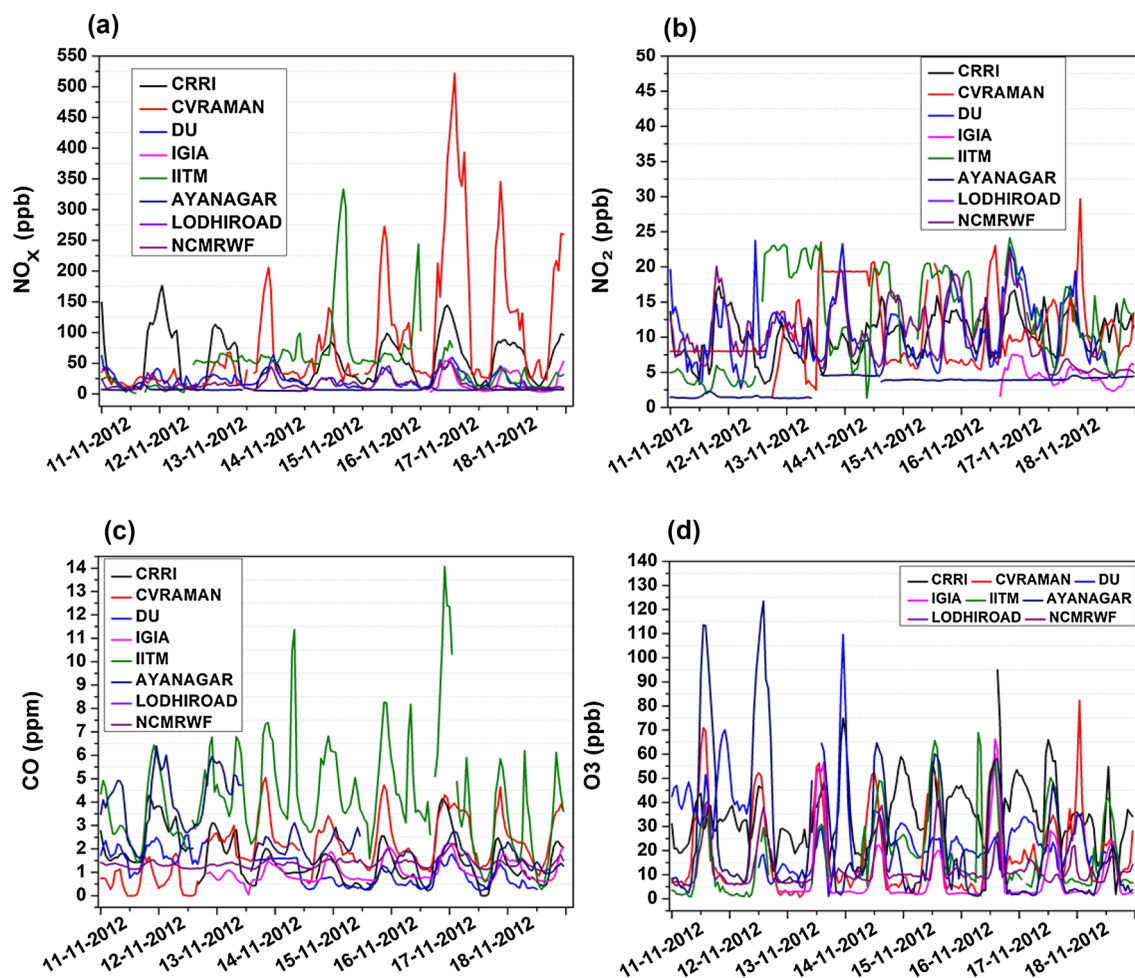


Fig. 8 Time series of air quality measurements over various location in New Delhi for a  $\text{NO}_x$ , b  $\text{NO}_2$ , c CO, and d  $\text{O}_3$

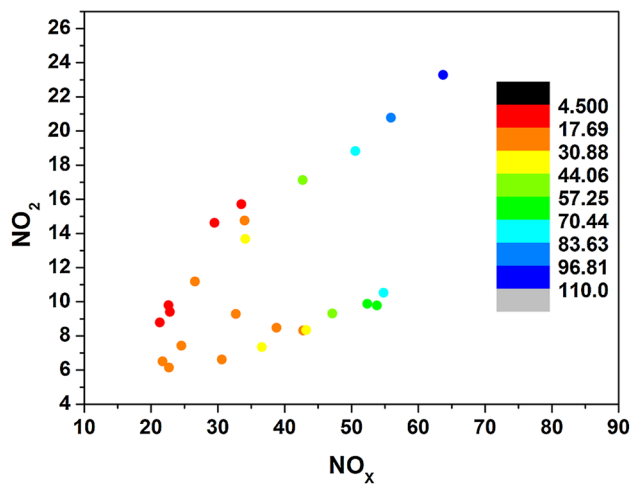


Fig. 9  $\text{NO}_x$  vs.  $\text{NO}_2$  by levels of ozone

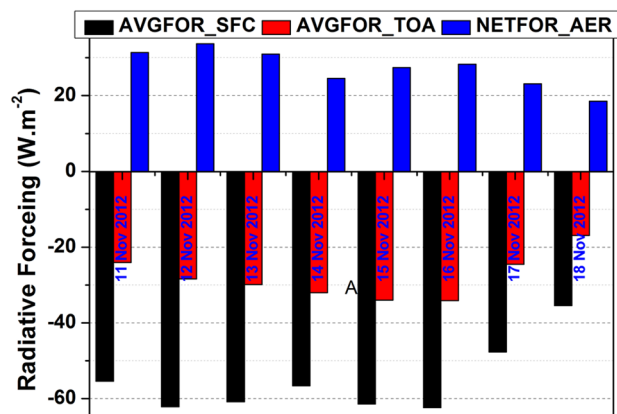


Fig. 10 Aerosol radiative forcing at surface, top of the atmosphere, and atmosphere during Diwali festival period

rate of 1.8 °C/day was estimated for the study period. The maximum average concentrations of PM<sub>10</sub> and PM<sub>2.5</sub> on Diwali night were observed as 2641 and 1876 µg/m<sup>3</sup>. It is also revealed that due to the burning of firecrackers, a highest amount of surface ozone (109 ppb) was perceived on 13th November at 23:00 IST. The anthropogenic activities during the Diwali period clearly illustrate drastic changes in aerosol optical and physical properties in a metropolitan city of NCR that can be directly effect on public health and radiative effects.

**Acknowledgements** The authors sincerely thank Dr. K. J. Ramesh, Director General of Meteorology, India Meteorology Department, for encouraging to carryout this work. We also acknowledge NOAA and NASA for providing online HYSPLIT back trajectory model and the MODIS L2 AOD products. We thank three anonymous reviewers for their constructive comments and suggestions which help us for further improvement in the manuscript.

## References

- Aksu A (2015) Sources of metal pollution in the urban atmosphere (a case study: Tuzla, Istanbul). *J Environ Health Sci Eng* 13(1):79–89
- Ali MA, Assiri M, Ramzah D (2017) Seasonal aerosol optical depth (AOD) variability using satellite data and its comparison over Saudi Arabia for the period 2002–2013. *Aerosol Air Qual Res* 17:1267–1280
- Angstrom A (1964) The parameters of atmospheric turbidity. *Eppley Found Res* 1:64–75
- Attri AK, Kumar U, Jain VK (2001) Microclimate formation of ozone by firecrackers. *Nature* 411(6841):1015
- Badarinath KVS, Kharol SK, Kaskaoutis DG, Sharma AR, Ramaswamy V, Kambezidis HD (2010) Long-range transport of dust aerosols over the Arabian Sea and Indian region—a case study using satellite data and ground-based measurements. *Global Planet Change* 72(3):164–181
- Barman SC, Singh R, Negi MPS, Bhargava SK (2008) Ambient air quality of Lucknow City (India) during use of firecrackers on Diwali Festival. *Environ Monit Assess* 137:495–504
- Bisht DS, Dumka UC, Kaskaoutis DG, Pipal AS, Srivastava AK, Soni VK, Tiwari S (2015) Carbonaceous aerosols and pollutants over Delhi urban environment: temporal evolution, source apportionment and radiative forcing. *Sci Total Environ* 521–522:431–445
- Chatterjee A, Sarkar C, Adak A, Mukherjee U, Ghosh SK, Raha S (2013) Ambient air quality during Diwali festival over Kolkata—a mega-city in India. *Aerosol and Air Quality Research* 13(13):1133–1144
- Clark H (1997) New directions light blue touch paper and retire. *Atmos Environ* 31(17):2893–2895
- Darga SS, Yogesh K, Mitra D (2006) Variability of aerosol optical depth and aerosol forcing over India. *Adv Space Res* 37(12):2153–2159
- Deng T, Deng X, Li F, Wang S, Wang G (2016) Study on aerosol optical properties and radiative effect in cloudy weather in the Guangzhou region. *Sci Total Environ* 568:147–154
- Devara PCS, Vijayakumar K, Safai PD, Raju MP, Rao PSP (2015) Celebration-induced air quality over a tropical urban station, Pune, India. *Atmos Pollut Res* 6:511–520
- Draxler RR (1998) An overview of the HYSPLIT\_4 modelling system for trajectories, dispersion, and deposition. *Aust Meteorol Mag* 47:295–308
- Dubovik O, King MD (2000) A flexible inversion algorithm for retrieval of aerosol optical properties from Sun and sky radiance measurements. *J Geophys Res* 105(D16):20673–20696
- Dumka UC, Saheb SD, Kaskaoutis DG, Kant Y, Mitra D (2016) Columnar aerosol characteristics and radiative forcing over the Doon Valley in the Shivalik range of northwestern Himalayas. *Environ Sci Pollut Res* 23(24):25467–25484
- Eck TF, Holben BN, Reid JS, Dubovik O, Smirnov A, O'Neill NT, Slutsker I, Kinne S (1999) Wavelength dependence of the optical depth of biomass burning, urban, and desert dust aerosols. *J Geophys Res* 104(D24):31333–31349
- Godri KJ, Green DC, Fuller GW, Dall'osto M, Beddows DC, Kelly FJ, Mudway IS (2010) Particulate oxidative burden associated with Firework activity. *Environ Sci Technol* 44(21):8295–8301
- Hoppel WA, Fitzgerald JW, Larson RE (1985) Aerosol size distributions in air masses advecting off the east coast of the United States. *J Geophys Res* 90(D1):2365–2379
- Jacobson MZ (2000) Implications for global direct forcing of aerosols Well-mixed. *Geophys Res Lett* 27(2):217–220
- Kaskaoutis DG, Sinha PR, Vinoj V, Kosmopoulos PG, Tripathi SN, Misra A, Singh RP (2013) Aerosol properties and radiative forcing over Kanpur during severe aerosol loading conditions. *Atmos Environ* 79:7–19
- Kaufman YJ, Setzen A, Ward D, Tanre D, Holben BN, Menzel P, Rasmussen R (1992) Biomass burning airborne and spaceborne experiment in the Amazonas (Base-a). *J Geophys Res Atmos* 97(D13):14581–14599
- Kharol SK, Badarinath KVS, Sharma AR, Mahalakshmi DV, Singh D, Prasad VK (2012) Black carbon aerosol variations over Patiala city, Punjab, India—a study during agriculture crop residue burning period using ground measurements and satellite data. *J Atmos Solar Terr Phys* 84:45–51
- Kulshrestha UC, Nageswara Rao T, Azhaguvel S, Kulshrestha MJ (2004) Emissions and accumulation of metals in the atmosphere due to crackers and sparkles during Diwali festival in India. *Atmos Environ* 38(27):4421–4425
- McCartney EJ, Hall FF (1977) Optics of the atmosphere: scattering by molecules and particles. *Phys Today* 30(5):76
- Mor V, Dhankhar R, Attri SD, Soni VK, Sateesh M, Taneja K (2017) Assessment of aerosols optical properties and radiative forcing over an Urban site in North-Western India. *Environ Technol* 38(10):1232–1244
- More S, Pradeep Kumar P, Gupta P, Devara PCS, Aher GR (2013) Comparison of aerosol products retrieved from AERONET, MICROTOS and MODIS over a Tropical Urban City, Pune, India. *Aerosol Air Qual Res* 13:107–121
- Nakajima T, Tonna G, Rao R, Boi P, Kaufman Y, Holben B (1996) Use of sky brightness measurements from ground for remote sensing of particulate polydispersions. *Appl Opt* 35(15):2672–2686
- Nichol JE, Bilal M (2016) Validation of MODIS 3 km resolution aerosol optical depth retrievals over Asia. *Remote Sens* 8:328
- Nidhi, Jayaraman G (2007) Air quality and respiratory health in Delhi. *Environ Monit Assess* 135:313–325
- Parkhi N, Chate D, Ghude SD, Peshin S, Mahajan A, Srinivas R, Beig G (2016) Large inter annual variation in air quality during the annual festival “Diwali” in an Indian megacity. *J Environ Sci (China)* 43:265–272
- Pervez S, Chakrabarty RK, Dewangan S, Watson JG, Chow JC, Matalwle JL (2016) Chemical speciation of aerosols and air quality degradation during the festival of lights (Diwali). *Atmos Pollut Res* 7(1):92–99

- Pongpiachan S, Hattayanone M, Suttinun O, Khumsup C, Kittikoon I, Hirunyatrakul P, Cao J (2017) Assessing human exposure to PM10-bound polycyclic aromatic hydrocarbons during firecrackers displays. *Atmos Pollut Res* 8(5):816–827
- Pöschl U (2005) Atmospheric aerosols: composition, transformation, climate and health effects. *Angew Chem Int Ed* 44:7520–7540
- Ramanathan V, Feng Y (2009) Air pollution, greenhouse gases and climate change: global and regional perspectives. *Atmos Environ* 43:37–50
- Ricchiazzi P, Yang S, Gautier C, Sowle D (1988) SBDART: a research and teaching software tool for plane-parallel radiative transfer in the earth's Atmosphere. *Bull Am Meteor Soc* 10:2101–2114
- Schaaf CB, Gao F, Strahler AH, Lucht W, Li X, Tsang T, Roy D (2002) First operational BRDF, albedo nadir reflectance products from MODIS. *Remote Sens Environ* 83(1–2):135–148
- Sharma AR, Kharo SK, Badarinath KVS, Singh D (2010) Impact of agriculture crop residue burning on atmospheric aerosol loading—a study over Punjab State, India. *Ann Geophys* 28(2):367–379
- Shaw GE (1988) Aerosol size-temperature relationship. *Geophys Res Lett* 15(2):133–135
- Simha CP, Devara PCS, Saha SK (2013) Aerosol pollution and its impact on regional climate during Holi festival inferred from ground-based and satellite remote sensing observations. *Nat Hazards* 69:889–903
- Singh RP, Dey S, Tripathi SN, Tare V (2004) Variability of aerosol parameters over Kanpur, northern India. *J Geophys Res* 109(D23):1–14
- Singh BP, Srivastava AK, Tiwari S, Singh S, Singh RK, Bisht DS, Srivastava MK (2014) Radiative impact of firecrackers at a tropical Indian location: a case study. *Adv Meteorol* 2014:1–8
- Singh A, Bloss WJ, Pope FD (2015) Remember, remember the 5th of November; Gunpowder, particles and smog. *Weather* 70(11):320–324
- Singh A, Bloss WJ, Pope FD (2017) 60 years of UK visibility measurements: impact of meteorology and atmospheric pollutants on visibility. *Atmos Chem Phys* 17(3):2085–2101
- Takemura T, Nakajima T (2002) Single-scattering albedo and radiative forcing of various aerosol species with a global three-dimensional model. *J Clim* 15(4):333–352
- Torres O, Bhartia PK, Herman JR, Ahmad Z, Gleason J (1998) Derivation of aerosol properties from satellite measurements of back-scattered ultraviolet radiation: theoretical basis. *J Geophys Res* 103(D14):17099–170110
- White AB, Senff CJ, Keane AN, Darby LS, Djalalova IV, Ruffieux DC, Goldstein AH (2006) A wind profiler trajectory tool for air quality transport applications. *J Geophys Res* 111(D23):1–11
- Zarzana KJ, Hann DOD, Freedman MA, Hasenkopf CA, Tolbert MA (2012) Optical properties of the products of  $\alpha$ -dicarbonyl and amine reactions in simulated cloud droplets. *Environ Sci Technol* 46(9):4845–4851